Soft X-ray laser observation of femtosecond-laser-driven ablation of tungsten

Masaharu Nishikino[1,*], Noboru Hasegawa[1], Masahiko Ishino[1], Yoshihiro Ochi[1], Tetsuya Kawachi[1], Mitsuru Yamagiwa[1], and Yoshiaki Kato[1,2,]**

[1]*Quantum Beam Science Directorate, Kansai Photon Science Institute, Japan Atomic Energy Agency, Kizugawa, Kyoto 619-0215, Japan*

[2]*Graduate School for the Creation of New Photonics Industries, Hamamatsu 431-1202, Japan*

**Corresponding author: nishikino.masaharu@jaea.go.jp; **corresponding author: y.kato@gpi.ac.jp*

Received April 19, 2015; accepted May 15, 2015; posted online June 11, 2015

Ablation dynamics of tungsten irradiated with a 70 fs laser pulse is investigated with X-ray interferometry and X-ray imaging using a 13.9 nm soft X-ray laser of 7 ps pulse duration. The evolution of high-density ablation front of tungsten (i.e., W) is presented. The ablation front expands to ~120 nm above the original target surface at 160 ps after femtosecond-laser irradiation with an expansion speed of approximately 750 m/s. These results will provide important data for understanding ablation properties of W, which is a candidate material of the first wall of magnetic confinement fusion reactors.

OCIS codes: 140.7240, 350.3390, 340.7440, 340.7450.

doi: 10.3788/COL201513.070002.

Quantum beam science is investigated at the Kansai Photon Science Institute (KPSI), Japan Atomic Energy Agency (JAEA). In the Institute's research, intense radiation such as X-ray and γ-ray radiation, high-power terahertz (THz) waves, and high-energy particles are generated with high-intensity lasers[1,2], and applications of these radiations to plasma physics[3,4], high-energy physics[5], industry, and medicine are developed. In this work we report on application of a soft X-ray laser to observation of ablation dynamics in tungsten (i.e., W) irradiated with a femtosecond (fs) laser.

Soft X-ray lasers[6] are very useful in various fields such as plasma physics[7], materials science[8], lithography, and biology. In plasma physics, dynamic processes in high-density plasmas can be observed with a soft X-ray laser due to its short wavelength, enabling propagation in high-density plasma, and short pulse duration. With picosecond-resolution interferometry using a soft X-ray laser, we have previously reported on observation of surface dilatation of Pt films due to ablation under fs laser irradiation[9]. Here we report on observation of ablation dynamics of W with fs laser irradiation using X-ray laser interferometry and imaging. Investigation of the ablation property of W is important since W is a candidate material of the first wall of magnetic confinement fusion reactors.

The amplification scheme of the Ag soft X-ray laser used in this work is shown in Fig. 1. The Ag atoms are ionized to Ni-like ions by irradiation of a weak laser pulse. The ground $3d^{10}$ state of the Ni-like Ag ion is then pumped to the $3d^9 4d$ excited state by electron collision with irradiation of an intense laser pulse. Population inversion between $3d^9 4d$ and $3d^9 4p$ is created due to rapid radiative decay of the $3d^9 4p$ state to the ground state, resulting in amplification of 13.9 nm radiation due to stimulated emission in the $3d^9 4d$–$3d^9 4p$ transition.

Figure 2 shows the layout of the soft X-ray laser. It is composed of an oscillator and an amplifier[10] which are separated by 20 cm. In the oscillator, a flat silver plate was irradiated with a 6.5 mm × 20 μm line-focused laser beam of 1.053 μm wavelength at an intensity of ~10^{15} W/cm^2. The laser pulse was composed of a 300 ps, 1 J prepulse and a 4 ps, 14 J main pulse with 600 ps delay. The wavefront of the pumping laser was tilted for travelling-wave amplification of the 13.9 nm radiation in the oscillator. The amplifier was irradiated under similar conditions with slightly less laser energy of 11 J.

By proper optimization of the mutual layout and the pumping timing between the oscillator and the amplifier, a small portion of the 6 mrad divergence X-ray laser beam from the oscillator was amplified in the amplifier with the energy gain of ~170, resulting in a monochromatic ($\Delta\lambda/\lambda \sim 10^{-4}$) soft X-ray laser beam with 270 nJ energy, 7 ps duration, and 0.2 mrad beam divergence, with almost full spatial coherence[11,12]. With this coherent soft X-ray laser, we have developed an X-ray laser interferometer

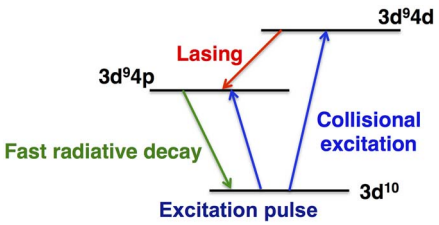

Fig. 1. Soft X-ray amplification with nickel-like Ag ions.

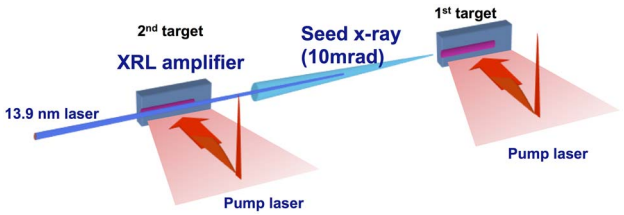

Fig. 2. Layout of a soft X-ray laser composed of an oscillator and an amplifier.

with lateral and depth resolutions of 1.5 μm and 1 nm, respectively[9,13].

The experimental arrangement of the X-ray laser interferometer for observing material ablation is shown in Fig. 3. A sample material (Pt, Au, or W) was evaporated on a fused silica substrate. The target was irradiated with a Ti:sapphire laser pulse (marked as pump pulse in Fig. 3) of 795 nm wavelength and 70 fs duration at an intensity of $\sim 3 \times 10^{13}$ W/cm^2 and energy density of ~ 2 J/cm^2. The ablation region was illuminated with the X-ray laser beam at a grazing angle of 22° and imaged with a Mo/Si-multilayer mirror with 19× magnification onto a CCD camera. Using a double Lloyd's mirror, a part of the X-ray laser beam which did not pass through the ablation region was reflected with a tilted grazing-incidence mirror and overlapped with the rest of the X-ray laser beam, forming the interference pattern in the overlapped region on the detector, as shown in the inset of Fig. 3.

The X-ray laser beam propagates through the low-density expanding plasma and is reflected at the boundary to the high-density region where material ablation is taking place. The profile of the ablation surface is determined by analyzing the fringe shifts of the interference pattern of the laser-irradiated region. By changing the time delay between the pumping pulse and the X-ray probe pulse, temporal evolution of the ablation surface is determined.

Figure 4(a) shows the interference patterns of the W surface at 48 and 71 ps after the fs laser irradiation. The temporal evolution of the ablation surface determined from analyses of the interference patterns is shown in Fig. 4(b). The nonuniform fringe shifts of the interference patterns reflect the profiles of the ablation front arising

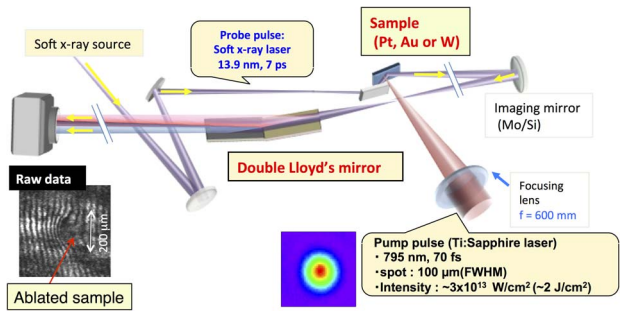

Fig. 3. X-ray laser interferometer using a double Lloyd's mirror for observation of ablation by fs laser irradiation. Inset, interference pattern with the fringe shift in the ablated region.

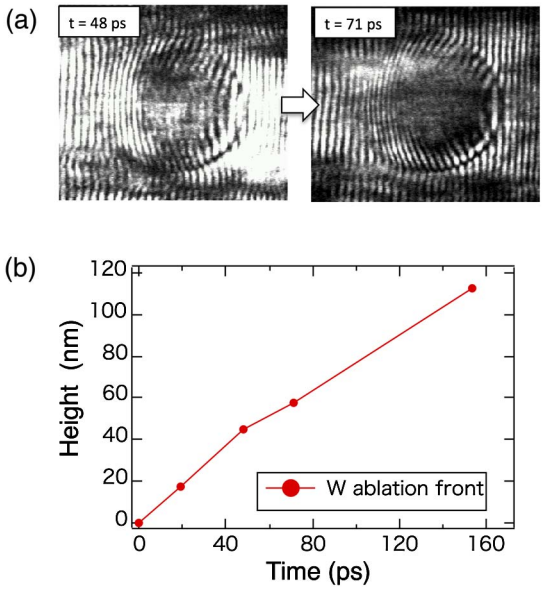

Fig. 4. (a) X-ray laser interference patterns of W at 48 and 71 ps after fs laser irradiation; (b) temporal evolution of the height of the ablation front, determined from the interference patterns.

from the spatial distribution of the pump laser irradiance on the target. From this observation we find that the ablation surface of W expands rapidly, reaching ~120 nm above the original surface at 160 ps, and gradually becomes lower at subsequent times. The expansion speed of the ablation front is approximately 750 m/s.

By removing the double Lloyd's mirror shown in Fig. 3, the arrangement of Fig. 3 was used to image the ablation region with the soft X-ray laser as the probe beam. Figure 5 shows the reflection images of the W surface at the delay

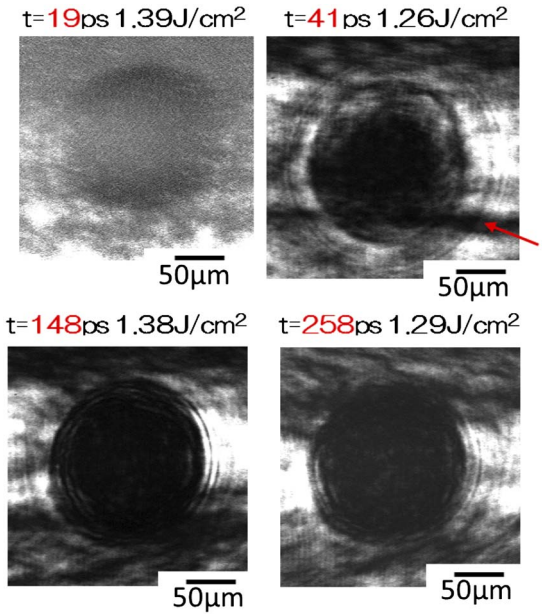

Fig. 5. X-ray reflective images of the ablation region of W ranging from 19 to 258 ps after fs laser irradiation.

times ranging from 19 to 258 ps after fs laser irradiation with fluence of 1.3–1.4 J/cm^2. The scale bar in Fig. 5 corresponds to 50 μm for all images, and the contrast was optimized for each image. The diameter of disk-shaped dark area gradually increases and reaches the maximum value at 260 ps, after which the diameter remains constant. These observed images with W can be compared with those with Pt[14].

The spatial variation of the reflectivity in these images indicates that the surface property depends strongly on the irradiation conditions. According to the X-Ray Database[15], the reflectivity reduces by more than 80% at the wavelength of 13.9 nm, when the surface roughness increases from 1 to 5 nm. This high sensitivity of the reflectivity to the surface roughness in the soft X-ray region will provide important information on the temporal roughness change of the ablation front which is caused, for example, by nanometer-scale bubble formation in the ablating high-density plasma. We have calculated the surface roughness of the ablation front, assuming that the density in the ablation region is close to the solid density and the reflectivity change is caused entirely by the surface roughness. The surface roughness of the ablation front thus estimated is approximately 5 nm.

We are studying the ablation properties of Au, Pt[9], and W under the same irradiation conditions. We find similarities and also differences of the ablation properties of these materials, providing interesting clues to understanding correlations between the ablation properties and the material parameters.

We note that W is a candidate material for the first wall of magnetic confinement fusion reactors. Studies of the ablation dynamics of reactor materials with plasma irradiation, often implemented for material evaluation, are complicated because the materials under the study are strongly mixed with the plasma particles. Since the present method of fs laser irradiation provides clear data which can be compared directly with molecular dynamic simulations[16], it will be valuable for understanding the ablation properties of W and other first wall materials when this approach is applied to them.

In conclusion, we demonstrate soft X-ray laser interferometry and imaging for observation of the initial phase of the ablation dynamics of W irradiated with a 70 fs laser pulse. The ablation front expands with the speed of approximately 750 m/s at the irradiation fluence of 1.3–1.4 J/cm^2. The surface roughness of the ablation front is estimated to be approximately 5 nm, indicating nanometer (nm)-scale nonuniformities in the ablating high-density plasma. This work will provide important data to evaluate the ablation processes of W, which is a candidate material for the first wall of magnetic confinement fusion reactors.

This work was partly supported by a Grant-in Aid for Scientific Research (Nos. 25390103 and 25289244) from the Japan Society for the Promotion of Science.

References

1. H. Kiriyama, M. Mori, A. S. Pirozhkov, K. Ogura, A. Sagisaka, A. Kon, T. Zh. Esirkepov, T. Hayashi, H. Kotaki, M. Kanasaki, H. Sakaki, Y. Fukuda, J. Koga, M. Nishiuchi, M. Kando, S. V. Bulanov, K. Kondo, P. R. Bolton, O. Slezak, D. Vojna, M. Sawicka-Chyla, V. Jambunathan, A. Lucianetti, and T. Mocek, IEEE J. Sel. Top. Quantum Electron. **21**, 1601118 (2015).
2. Y. Ochi, N. Hasegawa, T. Kawachi, and K. Nagashima, Appl. Opt. **46**, 1500 (2007).
3. A. S. Pirozhkov, J. Ma, M. Kando, T. Zh. Esirkepov, Y. Fukuda, L. M. Chen, I. Daito, K. Ogura, T. Homma, Y. Hayashi, H. Kotaki, A. Sagisaka, M. Mori, J. K. Koga, T. Kawachi, H. Daido, S. V. Bulanov, T. Kimura, Y. Kato, and T. Tajima, Phys. Plasmas **14**, 123106 (2007).
4. K. Ogura, M. Nishiuchi, A. S. Pirozhkov, T. Tanimoto, A. Sagisaka, T. Zh. Esirkepov, M. Kando, T. Shizuma, T. Hayakawa, H. Kiriyama, T. Shimomura, S. Kondo, S. Kanazawa, Y. Nakai, H. Sasao, F. Sasao, Y. Fukuda, H. Sakaki, M. Kanasaki, A. Yogo, S. V. Bulanov, P. R. Bolton, and K. Kondo, Opt. Lett. **37**, 2868 (2012).
5. M. Nishiuchi, H. Sakai, T. Zh. Esirkepov, K. Nishio, T. A. Pikuz, A. Ya. Faenov, I. Yu. Skobelev, R. Orlandi, H. Sako, A. S. Pirozhkov, K. Matsukawa, A. Sagisaka, K. Ogura, M. Kanasaki, H. Kiriyama, Y. Fukuda, H. Koura, M. Kando, T. Yamauchi, Y. Watanabe, S. V. Bulanov, K. Kondo, K. Imai, and S. Nagamiya, Phys. Plasmas **22**, 033107 (2015).
6. Y. Kato, "X-ray laser research: perspective and physics issues," in *Conference Series-Institute of Physics* (Institute of Physics, 2005), Vol. **186**, p. 3.
7. S. Magnitskiy, N. Nagorskiy, A. Faenov, T. Piluz, M. Tanaka, M. Ishino, M. Nishikino, Y. Fukuda, M. Kando, T. Kawachi, and Y. Kato, Nature Commun. **4**, 1936 (2013).
8. R. Z. Tai, K. Namikawa, M. Kishimoto, M. Tanaka, K. Sukegawa, N. Hasegawa, T. Kawachi, M. Kado, P. Lu, K. Nagashima, H. Daido, H. Maruyama, A. Sawada, M. Ando, and Y. Kato, Phys. Rev. Lett. **89**, 247602 (2002).
9. T. Suemoto, K. Terakawa, Y. Ochi, T. Tomita, M. Yamamoto, N. Hasegawa, M. Deki, Y. Minami, and T. Kawachi, Opt. Express **18**, 14114 (2010).
10. M. Nishikino and T. Kawachi, Nat. Photonics **8**, 352 (2014).
11. M. Tanaka, M. Nishikino, T. Kawachi, N. Hasegawa, M. Kado, M. Kishimoto, K. Nagashima, and Y. Kato, Opt. Lett. **28**, 1680 (2003).
12. M. Nishikino, M. Tanaka, K. Nagashima, M. Kishimoto, M. Kado, T. Kawachi, K. Sukegawa, Y. Ochi, N. Hasegawa, and Y. Kato, Phys. Rev. A **68**, 061802 (2003).
13. Y. Ochi, K. Terakawa, N. Hasegawa, M. Yamamoto, T. Tomita, T. Kawachi, Y. Minami, M. Nishikino, T. Imazono, M. Ishino, and T. Suemoto, Jpn. J. Appl. Phys. **51**, 016601 (2012).
14. T. Tomita, M. Yamamoto, N. Hasegawa, K. Terakawa, Y. Minami, M. Nishikino, M. Ishino, T. Kaihori, Y. Ochi, T. Kawachi, M. Yamagiwa, and T. Suemoto, Opt. Express **20**, 29329 (2012).
15. http://henke.lbl.gov/optical_constants.
16. B. J. Demaske, V. V. Zhakhovsky, N. A. Inogamov, and I. I. Oleynik, Phys. Rev. B **82**, 064113 (2010).